Fusion Engineering and Design 131 (2018) 21–28

Contents lists available at ScienceDirect

Fusion Engineering and Design

journal homepage: www.elsevier.com/locate/fusengdes

Electromagnetic force evaluation on the water cooled ceramic breeder blanket for CFETR

Xuebin Ma[a,b], Min Li[a], Songlin Liu[a,b,*]

[a] Institute of Plasma Physics, Chinese Academy of Sciences, Hefei, Anhui, 230031, China
[b] University of Science and Technology of China, Hefei, Anhui, 230027, China

ARTICLE INFO

Keywords:
Electromagnetic analysis
WCCB blanket
CFETR

ABSTRACT

The Water Cooled Ceramic Breeder (WCCB) blanket is one of the blanket candidates for Chinese Fusion Engineering Test Reactor (CFETR). To investigate the electromagnetic (EM) force (magnetization force and Lorentz force) on the WCCB blanket, EM analyses were carried out using ANSYS Multiphysics code. At first, finite element (FE) static magnetic analysis under normal operation condition was accomplished, adopting the magnetic scalar potential (MSP) method. The magnetization force can be obtained as a result. Then transient magnetic analysis under plasma disruption event was performed using the magnetic vector potential (MVP) method. The eddy current on blankets was subsequently analyzed. Finally, the Lorentz force applied on blankets can be calculated with cross-product of the eddy current field from transient magnetic analysis and the magnetic field from the static magnetic analysis. The EM forces will be used as mechanical loads for the future structural analysis of blanket under integrated load.

1. Introduction

As one of Chinese Fusion Engineering Test Reactor (CFETR) breeding blanket candidates, the Water Cooled Ceramic Breeder blanket (WCCB) concept [1] is being developed in Institute of Plasma Physics, Chinese Academy of Sciences (ASIPP). To investigate the mechanical performance of WCCB blanket under integrated load, it is necessary to calculate the electromagnetic (EM) forces, one of the important mechanical loads. EM forces are classified into two categories: the magnetization force and the Lorentz force. The magnetization force is caused by the magnetization of ferromagnetic material of blanket, namely reduced activation ferritic-martensitic (RAFM) steel. The Lorentz force is generated by the interaction between magnetic field and eddy current induced due to the variation of the magnetic flux through the structural components of blankets when an EM transient (e.g. plasma disruption event) happens. EM analyses were performed using ANSYS Multiphysics code to evaluate the EM forces on blankets. Static magnetic analysis and transient magnetic analysis of WCCB blankets were performed using the finite element (FE) magnetic scalar potential (MSP) method and the FE magnetic vector potential (MVP) method, respectively. The magnetization force can be obtained from the static magnetic analysis results using the virtual work method. A multiple-step method was proposed to calculate the Lorentz force. With cross-product of the eddy current field from transient magnetic analysis and the magnetic field obtained from the static magnetic analysis, the Lorentz force was calculated through Matlab programming.

2. Description of the WCCB blanket module

The WCCB blanket consists of first wall (FW), armor, cooling plates (CPs), stiffening plates (SPs), side walls (SWs), manifolds (MFs) and back plate (BP). The structure of the equatorial outboard blanket is shown in Fig. 1. The dimension of the blanket is 800 mm (radial) × 1482 mm (poloidal) × 950 mm (toroidal). The layout of the WCCB blanket employs the layered breeder outside the tube (BOT) design concept. The pebble bed is separated into 16 sub-modules by the FW, CPs, SWs and SPs. RAFM steel is employed as structural material. Tungsten armor acts as a plasma facing component to protect the FW from plasma thermal exposure, corrosion and erosion. Mixed pebble beds of Li_2TiO_3 and $Be_{12}Ti$ function as the tritium breeder and primary neutron multiplier, respectively. In addition, two thin layers of beryllium pebble bed are adopted as additional neutron multiplier to improve the neutronics performance.

* Corresponding author at: Institute of Plasma Physics, Chinese Academy of Sciences, Hefei, Anhui, 230031, China.
E-mail address: slliu@ipp.ac.cn (S. Liu).

https://doi.org/10.1016/j.fusengdes.2018.04.037
Received 3 November 2017; Received in revised form 26 March 2018; Accepted 9 April 2018
Available online 17 April 2018

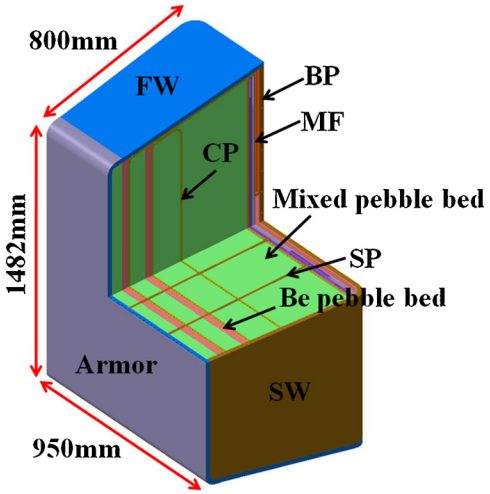

Fig. 1. The equatorial outboard WCCB blanket.

3. Static magnetic analysis for magnetization force

3.1. Finite element model

The 3D static magnetic analysis of WCCB blankets is performed using the ANSYS MSP formulation [2]. With the MSP formulation, current sources can be modeled as primitives rather than elements. The modeling of current sources can be simpler. Considering the periodicity of CFETR structure along the toroidal direction, 1/16 sector (22.5°) of the full model has been established. The FE model for static magnetic analysis consists of 25 blankets (15 outboard blankets and 10 inboard blankets), 16 toroidal field (TF) coils, 6 poloidal field (PF) coils, 6 center solenoid (CS) coils, the plasma, void and far field, as shown in Fig. 2. In addition, full model (360°) of current-carrying components is built according to ANSYS magnetic analysis rules. In view of the effect of magnetization of ferromagnetic material (structural material of blanket) on the magnetic field, 25 full models of blankets in the section are built in the FE model. All components of blankets, including FWs, CPs, SPs, SWs, BPs and pebble beds, are modeled in detail. As for the element type, SOLID96, SOURC36 and INFIN111 are employed for blanket components and void, current-carrying components (TF coils, PF coils, CS coils and the plasma) and far field, respectively. Solid96 is a scalar potential formulation element which is suitable for the calculation of 3D magnetic field in ferromagnetic material. SOURC36 is a primitive (consisting of predefined geometries) used to supply current source data to magnetic field problems and the element represents a distribution of current in a model employing a scalar potential formulation. TF coils, PF coils, CS coils and the plasma are modeled directly using SOURC36 without any geometric modeling and mesh generation. INFIN111 models an open boundary of a 3-D unbounded field problem. A single layer of elements is used to represent an exterior sub-domain of semi-infinite extent. The layer models the effect of far-field decay in magnetic analysis. Total 2,443,144 elements are generated for the FE model.

3.2. Material, loads and boundary conditions

The material adopted in the FE model includes void, RAFM steel, tungsten and pebble beds. The relative permeability of all the material is 1 except RAFM steel. The relative permeability of RAFM steel referred to F82H [3] is expressed through a B-H curve. The complex cooling channels and purge gas channels of blankets are filled with RAFM steel to reduce the difficulty in mesh generation and the amount of mesh. Due to the absence of channels in simulation model, the B-H curve for F82H steel should be corrected according to the following formula [4]:

$$B_{corr} = \mu_0 (H + \frac{V_{eff}}{V_{\mathrm{mod}}} M(H)) \quad (1)$$

where: B_{corr} is the corrected value of B in the F82H steel; μ_0 is the vacuum magnetic permeability; H is the magnetic field intensity; M is the magnetization intensity; V_{eff} is the steel volume in present simulation model; V_{mod} is the steel volume in the realistic model of blankets. The B-H curve for F82H steel and correction B-H curve for F82H steel in simulation model are shown in Fig. 3.

The loads for the simulation include the current density of TF coils, PF coils, CS coils and the plasma. All these loads are applied through the modeling of current-carrying components with SOURC36 element. The detailed parameters [5] are summarized in Table 1.

According to the periodicity of the model, cyclic symmetry boundary condition is applied on the opposite surfaces of the sector model, namely, the MAG degree of freedom (DOF) of nodes on the opposite surfaces is coupled. The flux parallel boundary condition is applied to the central axis of the model to simulate the direction of the magnetic field along the axis. Infinite field boundary condition is applied on the model by adding Infinite Surface Flags on the nodes at the outer surface to represent the unbounded field.

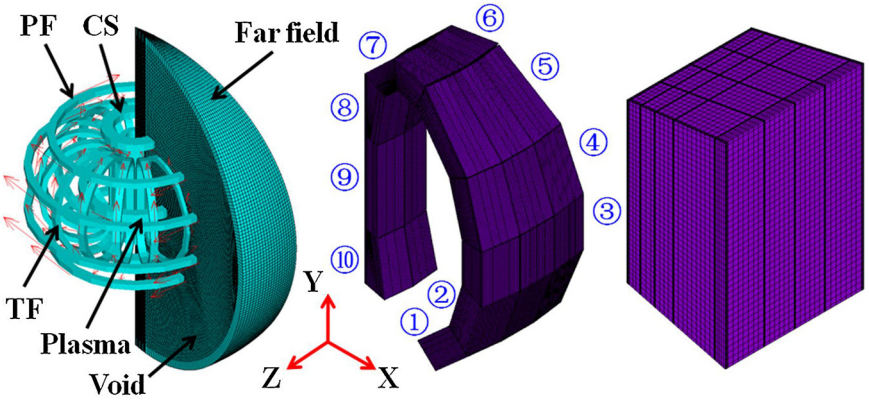

(a) overall model (b) all blankets (c) 3# blanket

Fig. 2. FE model for static analysis.

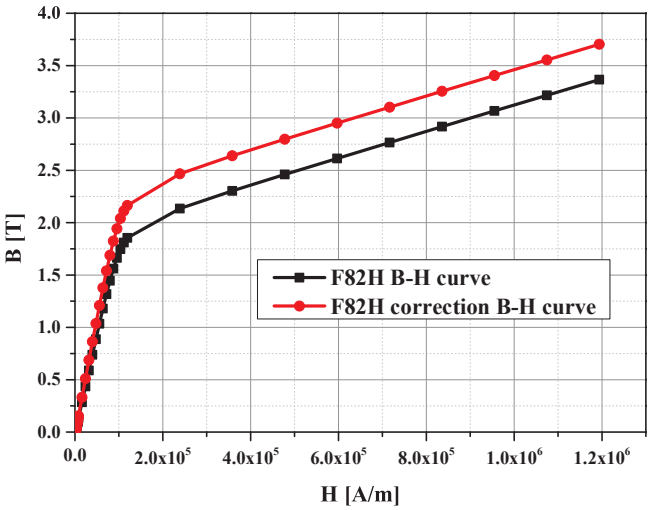

Fig. 3. B-H curve for F82H steel and correction B-H curve for F82H steel in simulation model.

Table 1
Design parameters of CFETR current-carrying components.

ITER-like coils	Currents (MA)
TF	8.897
PF1	9.240
PF2	−1.680
PF3	−4.704
PF4	−6.384
PF5	−0.504
PF6	6.160
CSU3	5.148
CSU2	−3.168
CSU1	−22.572
CSL1	−22.572
CSL2	2.772
CSL3	5.940
Plasma	10.000

3.3. Results and discussion

The magnetic field in CFETR is shown in Fig. 4. The peak value of magnetic flux density (10.4 T) appears at the equatorial section of CS coils due to the vector superposition of poloidal magnetic field generated by different coils. The magnetic flux density at the plasma center is 5.0 T, which is equal to the design parameters of CFETR coils [5]. Due to the magnetization of ferromagnetic material in high magnetic field, the blanket structural components induce an additional magnetic field, which is unnaturally enhanced the magnetic flux field on blanket area compared with the case without using RAFM steel. In contrast to other areas of blankets, there is a more significant increase of magnetic flux density on BPs of inboard blankets, probably due to its larger mass of RAFM steel than that of other components of blankets.

The magnetic field of the equatorial outboard blanket (3# blanket) is shown in Fig. 5 as an example. It is observed that the magnetic flux density on the CPs is higher than those on radial-poloidal plates. This is because CPs aligned with toroidal magnetic field is easily magnetized. As one of the two categories of EM forces, the magnetization forces on blanket are calculated based on the virtual work method. They can be conveniently calculated using a “FMAGSUM” macro in the post-processor of ANSYS, as shown in Fig. 6. The number of blankets and directions of magnetization forces (coordinate system) are shown in Fig. 2. The magnetization forces of inboard blankets are much larger than the outboard blankets. The magnetization force of 1123 kN appears on 9# blanket. It may be explained by the higher magnetic field

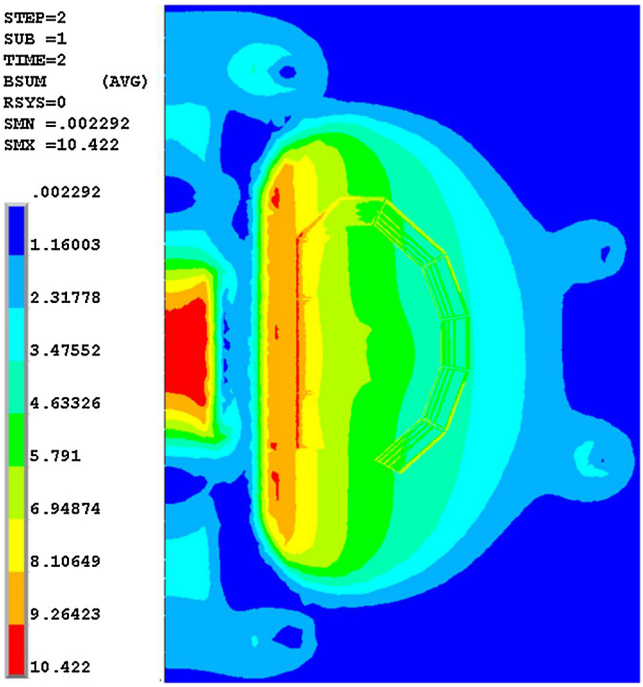

Fig. 4. Magnetic field in CFETR (poloidal-radial section view).

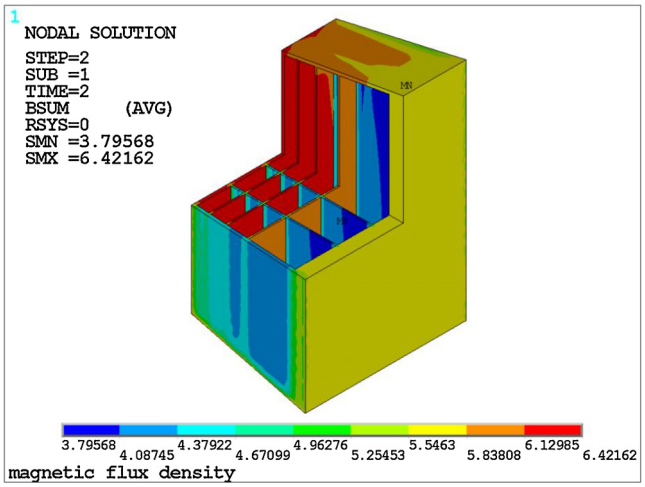

Fig. 5. Magnetic field in 3# blanket.

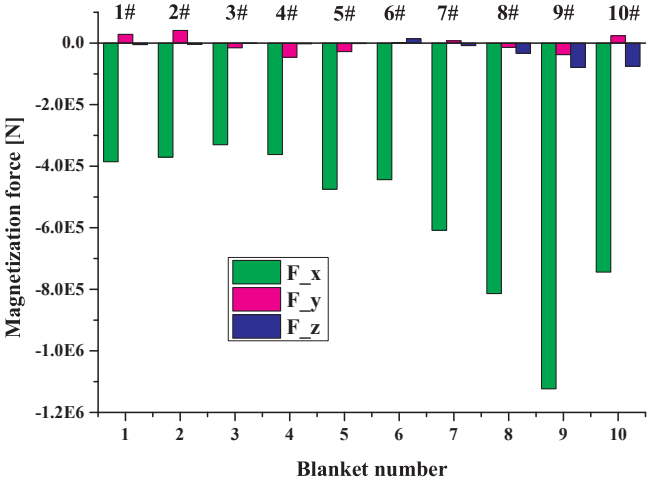

Fig. 6. Summary of magnetization forces of each blanket.

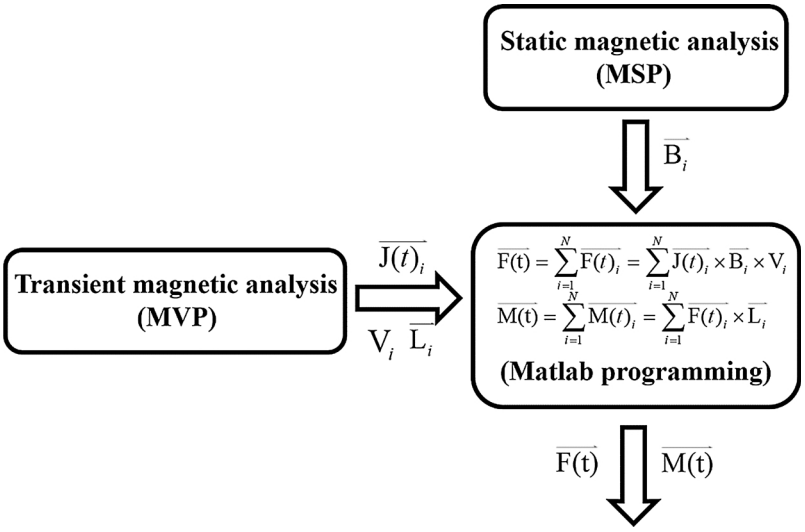

Fig. 7. The process flow chart of multiple-step method.

and larger volume of inboard blankets. Besides, the magnetization force along the X direction is dominant compared with the other two directions.

4. Transient magnetic analysis for Lorentz force

4.1. Plasma disruption event

Due to the lack of detailed plasma disruption simulation of CFETR, a 36 ms linear plasma disruption event and a 16 ms exponential plasma disruption event referring to ITER [6] were assumed for EM transient analyses. The plasma currents are expressed by formula (2) and formula (3), respectively.

$$I = I_0(1 - t/\tau) \tag{2}$$

$$I = I_0 e^{-t/\tau} \tag{3}$$

Where I is the plasma current; t is the time, the unit is ms. In formula (2), I_0 equals to 10 MA [5], τ equals to 36 ms. In formula (3), I_0 equals to 10 MA [5], τ equals to 16 ms.

4.2. Methodology for Lorentz force calculation

Transient magnetic analysis using the MVP formulation is performed for Lorentz force calculation. With the MVP formulation, current sources should be modeled as an integral part of the finite element model. Due to the added degrees of freedom (DOFs), the MVP formulation runs more slowly than the scalar formulation. When ferromagnetic material (RAFM steel) is included in the FE model, the solution is found to be inaccurate due to the significant normal component of the vector potential at the interface between elements of different permeability. Hence, a multiple-step method is proposed to calculate the Lorentz force through cross-product of the eddy current field obtained from transient magnetic analysis and the magnetic field in blanket. The procedure of the method is shown in Fig. 7. In the transient magnetic analysis, the MVP formulation is still adopted. The relative permeability of RAFM steel (F82H) is set to 1, namely, the nonlinearity of ferromagnetic material is neglected. In this way, the eddy current field in blankets can be obtained correctly. Then element solution of eddy current density is exported, together with the element volume and the arm of force of element. The arm of force is calculated based on a reference point located at the center of the reverse surface of the BPs. Because the magnetic field generated by TF coils, PF coils and CS coils doesn't change during the very short time of the plasma disruption event, the magnetic field in blankets for Lorentz force calculation during the plasma disruption event can be replaced by the magnetic field obtained in the static magnetic analysis. Finally, the Lorentz force and moment applied on the blanket are calculated according to formula (4) and formula (5).

$$\overrightarrow{F(t)} = \sum_{i=1}^{N} \overrightarrow{F(t)_i} = \sum_{i=1}^{N} \overrightarrow{J(t)_i} \times \overrightarrow{B_i} \times V_i \tag{4}$$

$$\overrightarrow{M(t)} = \sum_{i=1}^{N} \overrightarrow{M(t)_i} = \sum_{i=1}^{N} \overrightarrow{F(t)_i} \times \overrightarrow{L_i} \tag{5}$$

Where $\overrightarrow{F(t)}$ is the total Lorentz force on blanket, it changes with time; i is the number of element, N is the total number of element, $\overrightarrow{F(t)_i}$ is the Lorentz force of element i, $\overrightarrow{J(t)_i}$ is the eddy current density of element i, $\overrightarrow{B_i}$ is the magnetic field of element i, V_i is the volume of element i; $\overrightarrow{M(t)}$ is the total moment on blanket, $\overrightarrow{M(t)_i}$ is the moment on element i, $\overrightarrow{L_i}$ is the arm of force of element i, it is calculated based on a reference point located at the center of the reverse surface of the BPs.

4.3. Finite element model

The 3D transient magnetic analysis of WCCB blankets is performed using the ANSYS MVP formulation [2]. FE model of a 22.5° sector of CFETR has been built. The model consists of 25 blankets (15 outboard blankets and 10 inboard blankets), vacuum vessel (VV), the plasma, void and far field, as shown in Fig. 8. To obtain more accurate eddy current, all components of blankets, including FWs, CPs, SPs, SWs, MFs, BPs and pebble beds, are modeled in detail. Because the current spatial distribution of plasma for CFETR remains unknown so far. The plasma is modeled as a cylinder current source with even current distribution as a simplified model. The current source is located at the center of vacuum vessel. TF coils, PF coils and CS coils are not included in the model because the magnetic field generated by these current-carrying components remain unchanged during the very short time of the plasma disruption event. As for the element type, SOLID97 and INFIN111 are

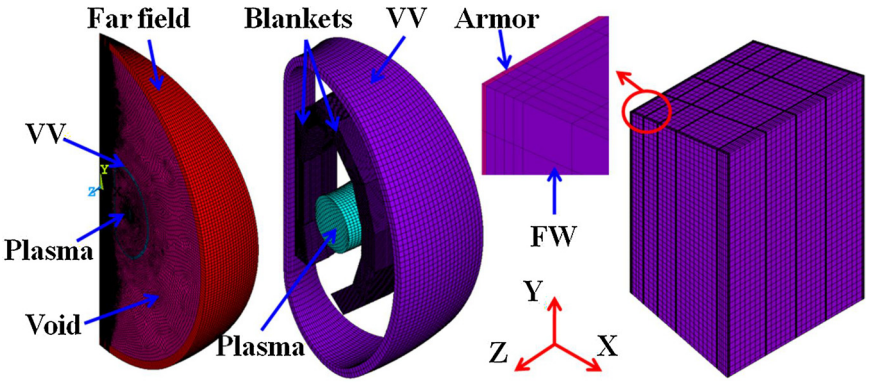

(a) overall model (b) blankets/plasma/VV (c)3# blanket

Fig. 8. FE model for transient analysis.

Table 2
Element type for transient analysis.

Element type	Component
Solid97, KEYOPT (1) = 0	Plasma, void, pebble beds of blankets
Solid97, KEYOPT (1) = 1	VV, W armor/structural components of blankets
Infin111	Far field

employed, as listed in Table 2. Total 7,329,213 elements are generated for the FE model. In particular, two simulation cases are set up to study the effect of material with low electrical resistivity (tungsten) on eddy current field and Lorentz force:

Case I. the tungsten armor is not included in FE model of 3# blanket.

Case II. the tungsten armor is included in FE model of 3# blanket.

4.4. Material, loads and boundary conditions

According to the components included in the FE model, the material adopted in the model includes RAFM steel, tungsten, SS316, void and pebble beds. The electrical conductivity of pebble beds has not been taken into consideration in the study. The complex cooling channels and purge gas channels in blankets are filled with RAFM steel (F82H steel) to simplify the model. The resistivity of the simplified structural components is expressed by the effective resistivity according to the following formula [3]:

$$\rho_{eff} = \rho \frac{S_{eff}}{S_{\mathrm{mod}}} \tag{6}$$

where: ρ_{eff} is the effective resistivity of F82H steel; ρ is the resistivity of F82H steel; S_{eff} is the steel section area in present simulation model; S_{mod} is the steel section area in the realistic model of blankets. The resistivity parameters of material [7–9] are listed in Table 3.

The plasma current is the only load for the transient analysis, as shown in formula (2) and formula (3). The following boundary conditions are applied on the FE model: (1) According to the periodicity of the model, cyclic symmetry boundary condition is applied on the opposite surfaces of the sector model; (2) The flux parallel boundary condition is applied to the central axis of the model to simulate the direction of the magnetic field along the axis; (3) Infinite field boundary condition is applied on the nodes at the outer surface to represent the unbounded field; (4) The BPs of blankets connect with ground.

4.5. Eddy current results

The eddy current field in all blankets are obtained through the transient analysis. They are input data for the Lorentz force calculation on blankets. The eddy current field in 3# blanket (case I) under 36 ms linear plasma disruption event is shown in Fig. 9 as an example. The eddy current flows along the radial-toroidal-radial-toroidal direction, namely it flows around the magnetic induction lines generated by the plasma current. The eddy current density in SWs and armor is much higher than the other components. The maximum eddy current density of 3# blanket over time under the 36 ms linear plasma disruption event is shown in Fig. 10. In case I, the maximum eddy current density appears in the SWs. In case II, the maximum eddy current density appears in the armor. The eddy current in the armor is about one order of magnitude higher than the eddy current in the SWs. It is caused by the much better electrical conductivity of tungsten compared with RAFM steel and the plate type structure of the armor adopted in FE model. The

Table 3
Resistivity parameters of model components.

Component	Material	Working temperature (°C)	Resistivity (Ω·m)	Eqv resistivity (Ω·m)
FW	F82H	400	7.58E-7	8.82E-7
CP	F82H	300	6.69E-7	8.03E-7
SP	F82H	300	6.69E-7	7.51E-7
SW	F82H	300	6.69E-7	7.23E-7
BP	F82H	300	6.69E-7	8.62E-7
Armor	Tungsten	400	1.50E-7	–
VV	SS316	20	7.40E-7	–

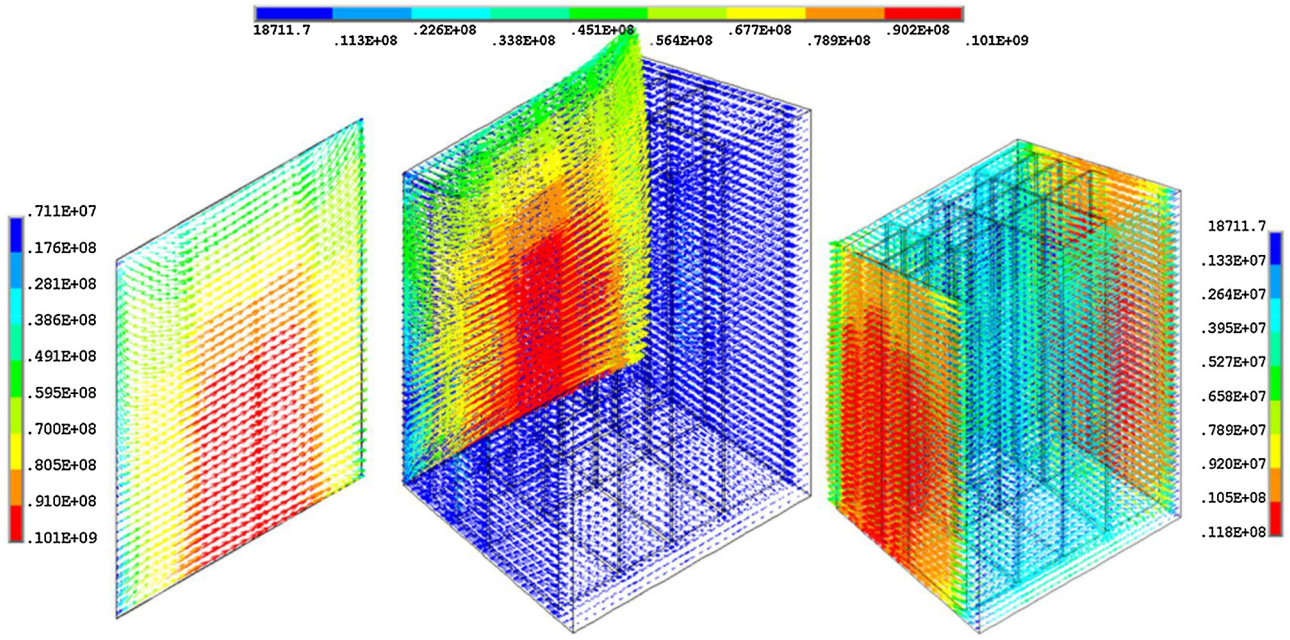

Fig. 9. Eddy current field in 3# blanket (time = 36 ms) under 36 ms linear plasma disruption event.

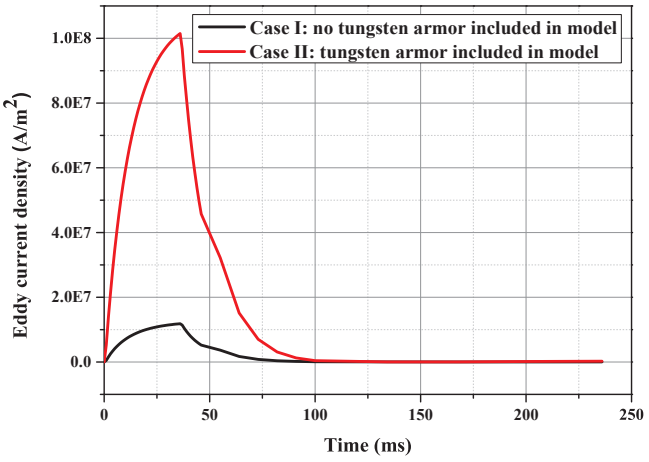

Fig. 10. Max eddy current density of 3# blanket vs time under 36 ms linear plasma disruption event.

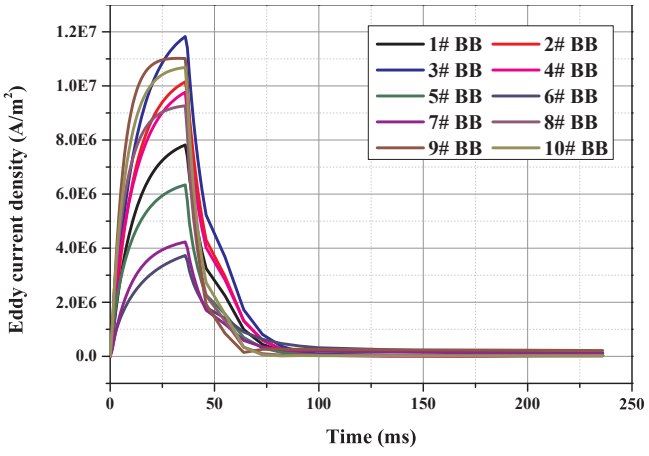

Fig. 11. Max eddy current density of blankets vs time under 36 ms linear plasma disruption event for case I.

enormous eddy current in the armor may affect the Lorentz force applied on blanket greatly. It is possible for the tungsten armor designed as the castellated tiles to reduce eddy current.

According to the simulation results in case I, the maximum eddy current density of all blankets over time under the 36 ms linear plasma disruption event and the 16 ms exponential plasma disruption event are shown in Fig. 11 and 12, respectively. In Fig. 11, the eddy current density increases sharply at an early stage of the plasma disruption event and reaches a peak at the time of 36 ms. Then the eddy current density decreases sharply and becomes around zero at the time of 100 ms. The maximum eddy current density of 2# blanket, 3# blanket, 4 # blanket, 8# blanket, 9# blanket and 10# blanket is much larger than the other blankets. The curves of the maximum eddy current density under the 16 ms exponential plasma disruption event are similar. The peak value of eddy current density occurs at the time of about 11 ms.

4.6. Lorentz force calculation

The Lorentz force acted on blanket is calculated based on the multiple-step method. The Lorentz force of 3# blanket under 36 ms linear plasma disruption event and the 16 ms exponential plasma disruption event are shown in Fig. 13. The Lorentz force along the Z direction (F_z) remain near zero during the plasma disruption event due to the

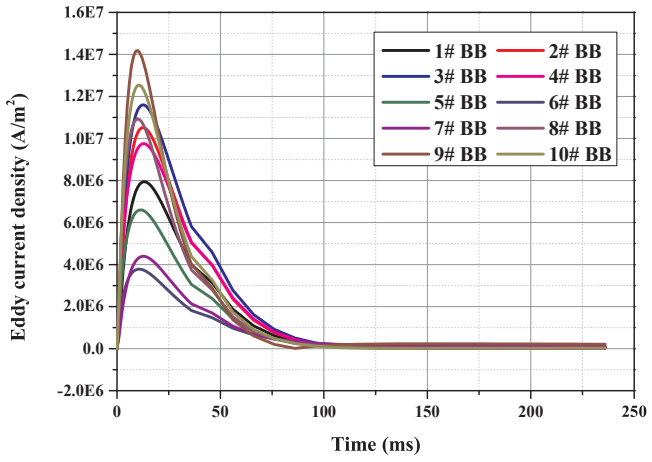

Fig. 12. Max eddy current density of blankets vs time under 16 ms exponential plasma disruption event for case I.

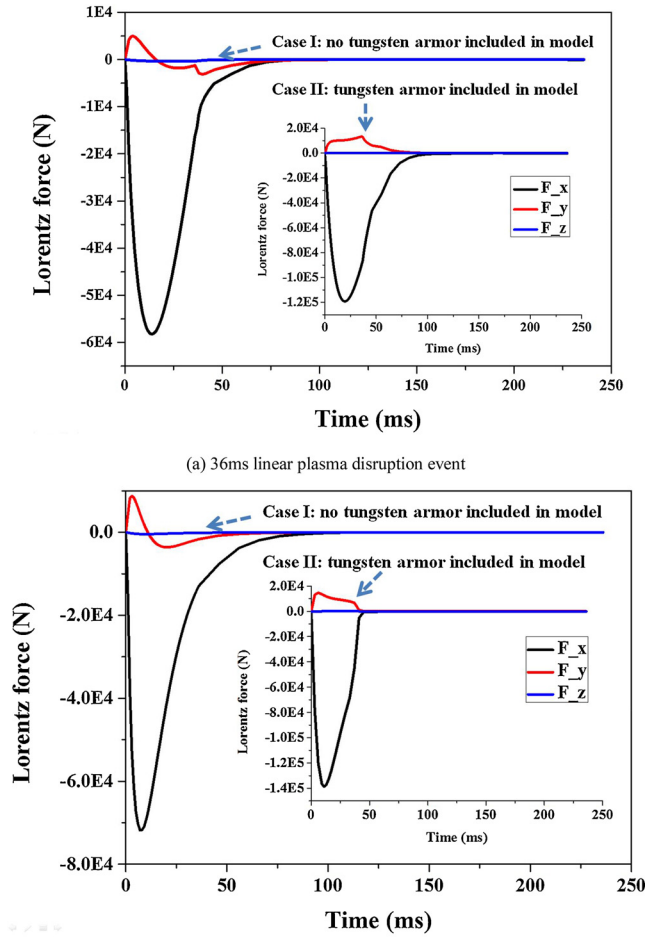

(a) 36ms linear plasma disruption event

(b) 16 ms exponential plasma disruption event

Fig. 13. Lorentz force of 3# blanket versus time.

symmetric location and symmetric structure of 3# blanket. The Lorentz force along the X direction (F_x) are dominant compared with F_y and F_z. It increases sharply at an early stage of the plasma disruption event and reaches a peak. Then it decreases to zero at the time of 100 ms. During the 36 ms linear plasma disruption event, F_x reaches the peak of 58,221 N at the time of 14 ms in case I, F_x reaches the peak of 119,170 N at the time of 19 ms in case II. During the 16 ms exponential plasma disruption event, F_x reaches the peak of 71823 N at the time of 7 ms in case I, F_x reaches the peak of 138,540 N at the time of 11 ms in case II. Due to the existence of tungsten armor in FE model of 3# blanket, the maximum Lorentz force of 3# almost doubles. So it is necessary to take the tungsten armor into consideration to evaluate the Lorentz force on blankets correctly in future FE simulation. Corresponding to the time when the maximum F_x occurs, the Lorentz forces on components of 3# blanket are summarized in Table 4 (tungsten armor is included in 3# blanket).The table shows enormous Lorentz forces are applied on armor, FW, SW and BP. Especially, the maximum Lorentz force acted on armor reaches up to271 kN. Due to the relatively weak structure, mechanical performance of the interface between armor and FW considering EM force should be pay attention to.

It has been proved that the tungsten armor has a significant impact on the Lorentz force of blanket. However, tungsten armors are not taken in consideration in FE models of blankets (except for 3# blanket) in the simulation. The effect of tungsten armor on Lorentz force has been quantified through the comparison between the Lorentz forces on 3# blanket calculated in case I and case II. A gain in the resultant Lorentz force of about + 119% under the 36 ms linear plasma disruption event and 107% under the 16 ms exponential plasma disruption event due to the effect of the addition of tungsten armor in FE model has been estimated. The resultant Lorentz force of the other blankets (except for 3# blanket) can be calculated according to correction factor of the + 119% and 107% for 36 ms linear plasma disruption event and 16 ms exponential plasma disruption event, respectively. The resultant Lorentz forces of all blankets under both of the plasma disruption events are shown in Fig. 14(a) and (b), respectively. The resultant Lorentz force of each blanket increases sharply first, then it reaches a peak and decreases sharply to zero. For different blankets, the corresponding time of peak value is different. The maximum resultant Lorentz force on blanket are summarized in Table 5. The maximum resultant Lorentz forces on 9# blanket and 3# blanket are much larger than the other blankets due to the combined effect of larger eddy current field, magnetic field and the volume of blankets.

5. Summary

The static and transient magnetic analyses have been carried out. The EM force acted on 1# blanket ~ 10# blanket surrounding the plasma are obtained.

The magnetization forces of inboard blankets are much larger than the outboard blankets. The magnetization forces on blankets along the radial direction are dominant compared with the toroidal direction and poloidal direction. The magnetization force on 9# blanket along the radial direction is 1123 kN. The magnetization force on 3# blanket along the radial direction is 330 kN.

The effect of tungsten armor on Lorentz force has been identified through the comparison between the Lorentz forces on 3# blanket calculated in FE model with/without tungsten armor. It has been found that enormous Lorentz force is applied on tungsten armor. Under the 36 ms linear plasma disruption event and the 16 ms exponential plasma disruption event, the maximum Lorentz force on armor of 3# blanket is about 224 kN and 271 kN, respectively, and a gain factor of about 119% and 107% are estimated when the tungsten armor is modeled in FE model. The tungsten armor has a significant impact on the Lorentz force on blanket. According to the gain factor, the maximum Lorentz force on 9# blanket is 509.6 kN and 590 kN for both events, respectively.

The Lorentz force on armor is one of the most important factors in

Table 4
Summary of maximum Lorentz force on components of 3# blanket.

	36 ms linear plasma disruption event			16 ms exponential plasma disruption event		
	F_x [kN]	F_y [kN]	F_z [kN]	F_x [kN]	F_y [kN]	F_z [kN]
Armor	−224.4	−26.0	0.1	−271.3	−32.2	0.2
FW	−189.3	−7.1	−0.8	−219.3	−7.5	−0.9
CP1	−69.7	−5.8	−0.02	−80.0	−6.7	−0.03
CP2	−35.0	−2.6	−0.04	−35.2	−2.6	−0.05
CP3	−4.9	−0.04	−0.01	−0.3	−0.5	−0.01
CP4	43.0	2.9	0.02	48.5	3.3	0.02
SW_left	−118.3	624.2	376.5	−148.2	728.4	446.5
SW_right	74.3	−625.7	−390.7	96.1	−730.3	−464.7
SP1	15.1	−134.0	−90.2	18.5	−146.9	−101.5
SP2	−1.4	−0.1	−0.05	−1.4	−0.1	−0.05
SP3	−17.6	133.3	88.6	−21.1	146.2	99.5
BP	479.5	24.1	−0.2	555.1	29.4	−0.2

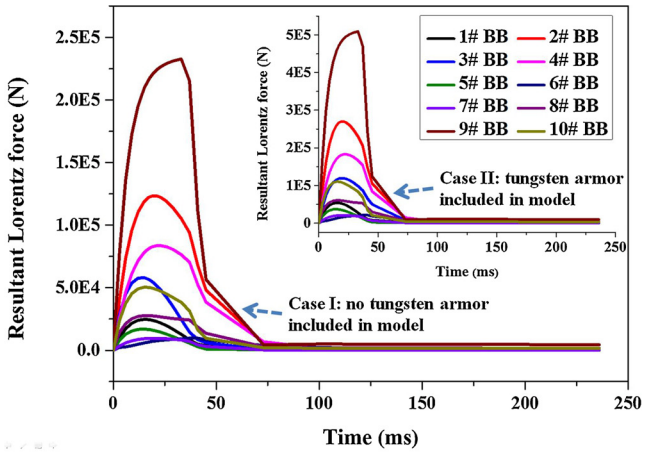

(a) 36ms linear plasma disruption event

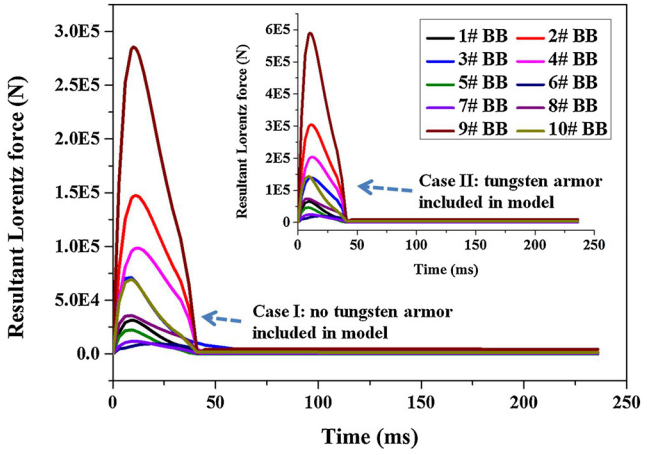

(b) 16 ms exponential plasma disruption event

Fig. 14. Resultant Lorentz force of all blankets versus time.

the design and manufacturing of armor. In order to reduce Lorentz force on armor, the castellated tile structure [10] is recommended for the tungsten armor. However, it would be necessary to investigate how the size of the tungsten castellated tiles impact on the Lorentz force on blanket.

Table 5
Summary of maximum resultant Lorentz force on blankets.

	36 ms linear plasma disruption event		16 ms exponential plasma disruption event	
Tungsten armor included or not	No (case I)	Yes (case II)	No (case I)	Yes (case II)
	F [kN]	F [kN]	F [kN]	F [kN]
1#	24.7	54.1	31.6	65.2
2#	123.4	270.2	147.4	304.6
3#	54.7	119.6	67.4	139.1
4#	83.7	183.3	98.6	203.6
5#	16.9	37.0	22.4	46.2
6#	9.7	21.2	9.5	19.6
7#	9.6	21.0	11.9	24.5
8#	27.7	60.7	35.7	73.8
9#	232.7	509.6	285.7	590.0
10#	50.4	110.4	69.5	143.6

Acknowledgements

This work was supported by the National Magnetic Confinement Fusion Science Program of China under Grants No. 2013GB108004, No. 2015GB108002 and Project funded by China Postdoctoral Science Foundation No. 2016M592074.

References

[1] S. Liu, et al. Conceptual design of the water cooled ceramic breeder blanket for CFETR based on pressurized water cooled reactor technology, Fusion Engineering and Design, https://doi.org/10.1016/j.fusengdes.2017.02.065.
[2] ANSYS 14.5, User Manual, ANSYS, 2014.
[3] F. Tavassoli, Fusion Demo Interim Structural Design Criteria (DISDC)/Appendix A: Material Design Limit Data/A3. S18E Eurofer Steel, (2004).
[4] R. Roccella, et al., Assessment of EM loads on the EU HCPB TBM during plasma disruption and normal operating scenario including the ferromagnetic effect, Fusion Eng. Des. 83 (2008) 1212–1216.
[5] Weiwei Xu, et al., Multi-scenario electromagnetic load analysis for CFETR and EAST magnet systems, Fusion Eng. Des. 114 (2017) 131–140.
[6] Load Specifications (LS), ITER_D_222QGL v6.2, (2017).
[7] Takanori Hirose, et al., Physical properties of F82H for fusion blanket design, Fusion Eng. Des. 89 (2014) 1595–1599.
[8] ITER MATERIAL PROPERTIES HANDBOOK, ITER Document NO. S74MA2, File Code: ITER-AM01-3201.
[9] ITER MATERIAL PROPERTIES HANDBOOK, ITER Document NO. S74MA2, File Code: ITER-AA01-3201.
[10] S.-H. Hong, et al., Castellated tungsten plasma-facing components exposed to H-mode plasma in KSTARS, Fusion Eng. Des. 109–111 (2016) 872–877.